Study of the Solar Performance of a Solar Refrigerator Using a Silica Gel-water Combination

Abstract :

The objective of this work is to contribute to a better understanding of the working of the refrigeration systems by adsorption. An experimental survey is led on such a prototype using silicagel-water couple constructs by BLM and installed in Ouagadougou (IRSAT) in the eighty years. It comes out again that the COPs of this machine varies between 0,091 and 0,138 for an irradiation solar daily average understood between 14,56 MJ and 18,68 MJ. This prototype, despite its old age has an interesting COPs and testify an increase of the temperature to the evaporator in relation to the one foreseen initially.

Keywords: Adsorption Refrigeration, Silicagel-water, solar energy, Solar performance coefficient, experimental.

Introduction

Usually, cold is obtained using compression systems, which require enormous amounts of energy to operate [1]. These systems use refrigerants such as chlorofluorocarbons (CFCs), hydrochlorofluorocarbons (HCFCs) and hydrofluorocarbons (HFCs), which are responsible for ozone depletion[2]. As a result, these systems contribute to climate change through the combined effect of refrigerant emissions and the resulting increase in greenhouse gas emissions.

In this context, adsorption refrigeration systems are a good alternative because they produce cold using renewable energy sources, particularly solar energy. In addition to being a simple technology, these adsorption refrigeration systems offer an alternative solution for both the environment and countries with high levels of sunshine. However, these adsorption refrigeration systems have been the subject of intense research over the last decade, and prototypes have been designed[1],[3],[4]. In fact, we can cite the following projects:

Boubakri et al (1992) [5] have designed a solar adsorption refrigeration system using a tubular adsorber collector operating with activated carbon/methanol. This prototype was tested in the meteorological conditions of Agadir (Morocco). It achieved evaporator temperatures of -6°C. Their experimental results showed that the solar COP varied between 0,08 and 0,12.

In Switzerland, Hildbrand et al (2005) developed a prototype solar refrigerator using a single-glazed flat-plate solar collector and a silica gel-water couple[6] . This adsorber-collector is

equipped with ventilation flaps that allow night-time cooling and promote adsorption. This cooling system performed well, with a solar COP of 0,16.

Bouzeffour et al, (2016) [7] have developed and tested a solar refrigeration system with the adsorption process operating with the silicagel/water couple. Their prototype uses a single-glazed flat-plate solar collector. The minimum temperature reached in the evaporator is around +5°C. The experimental solar COP obtained with the prototype during the test period varies from 0.083 to 0.09 under the climatic conditions of Bou-Ismail (Algeria).

The aim of this work is to contribute to a better understanding of the operation of adsorption refrigeration systems through an experimental study of the BLM prototype under the climatic conditions of Ouagadougou.

1. Material and methods

1.1. Study area

The prototype we studied was installed in Burkina Faso (Ouagadougou) at a latitude of 12°22’30.31’’ and a longitude of 01°29’53.31’’. The prototype, manufactured by the Brissoneau and Lotz-Marine (BLM) laboratory, consists of two adsorber sensor, a condenser and an evaporator housed in the refrigeration chamber. To carry out the work, the temperature and solar radiation measurements were carried out in June and July. During this period, the sky in Ouagadougou is less full of dust particles.

Figure 1: Photo of the adsorption solar refrigerator

1.2. How the adsorption solar refrigerator works

This system operates on an intermittent cycle basis. The intermittence of the solar adsorption refrigerator's cold production cycle is synchronized with that of the solar energy source. Thus, the operating principle of these systems is based on the thermodynamic cycle, which can be summarized as follows:

- Daytime heating phase

From 1 to 2 (isostere), the adsorber is isolated. Under the event of heat, the pressure and temperature of the mixture increase, while the total mass of refrigerant adsorbed remains constant and equal to m_{max} . This pressurization phase ends as soon as the pressure equals that in the condenser P_c (point 2), where $P_c = P_s(T_c)$.

From 2 to 3 (desorption-condensation), the adsorber is brought into contact with the condenser and refrigerant desorption begins. The adsorber is now at a pressure equal to the condensation pressure, and follows the isobaric pressure imposed by the condenser. As heating continues, the temperature of the mixture in the adsorber will rise to the maximum temperature T_g.

- Night-time cooling phase

From 3 to 4 (isostere), the adsorber is again isolated. Cooling of the adsorbent/adsorbate mixture begins at point 3, where temperature and pressure decrease until the pressure is equal to that in the evaporator $P_e = P_s(T_e)$. The temperature reached is called the adsorption "threshold temperature" T_{c2} (point 4). The total mass of fluid adsorbed is constant at this stage, equal to m_{min} .

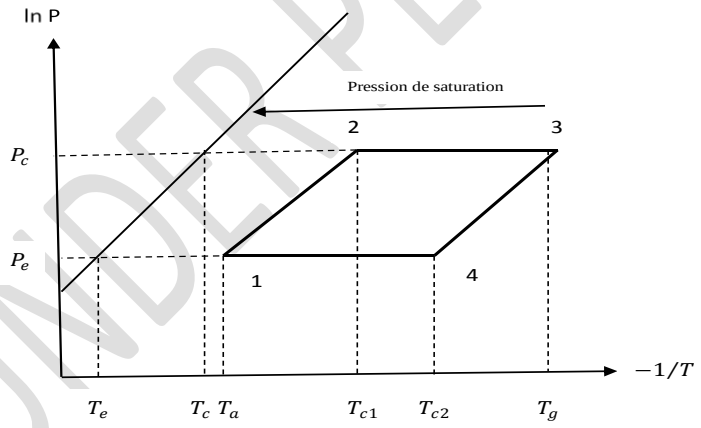

Figure 2: Ideal cycle of an adsorption Solar refrigerator

1.3. Protocole expérimental

The study of the adsorption solar refrigerator requires knowledge of data such as the temperature of its various parts and the amount of sunshine. For temperature measurement, K-type thermocouples are used with an accuracy of 1%. The pyranometer type "sensor basic including irradiance sensor and module temperature sensor" is also used. K-type thermocouples are placed on each part, and a pyranometer is placed on the glass at the same

angle as the glass. These are then connected to a data logger, enabling data to be recorded automatically over a five-second time interval. This results in the following diagram.

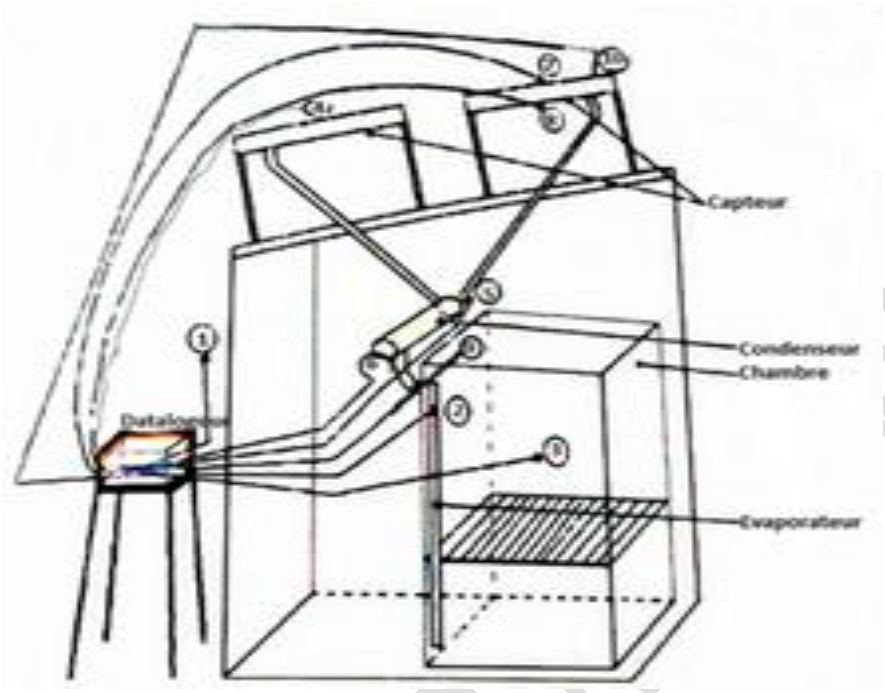

Figure 3: Experimental set-up

1.4.Uncertainty analysis

Every possible care and precaution is taken in the conduct of the experimental work, but errors do occur in the measurement of various parameters. This may occur due to the large number of instruments used in the experiment. As a result, it is estimated that there may be inaccuracies in measurement during the course of the experimental work. The total measurement uncertainty is defined as the difference between the quantity measured and its value. The uncertainty analysis performed by Kline and McClintock was used to estimate the uncertainty associated with the present study. Consequently, the uncertainty analysis was carried out using the experimental results obtained from the present study. The error values of various parameters for the present experimental work are given in the table.

Table 1. The measures, symbols and Uncertainty.

N°	Measure	Symbol	uncertainty
1	Ambient temperature	T_{amb} [°C]	$\pm$ 1.5
2	Sensor temperature	T_{cap} [°C]	$\pm$ 2.6
3	Condenser temperature	T_c [°C]	$\pm$ 1.95

4	Evaporator temperature	T_e [°C]	$\pm$ 3.23
5	Solar radiation	I_g $[W/m^2]$	$\pm$ 0.38

1.5. Solar coefficient of performance calculation (COPs)

The solar coefficient of performanceCOP_s of the adsorption solar refrigerator studied is given by the following relationship:

$$COP_s = \frac{Q_f}{I_g}$$

I_g : is the solar energy received by the collector-adsorber.

$$I_g = A * \int_{t_l}^{t_s} I(t)dt$$

A: collector area in m^2;

I(t): hourly solar irradiance in w/s

Q_f : is the amount of heat extracted from the evaporator:

$$Q_f = m_{ad}\left[L(T_e) - C_{pa}(T_c - T_e)\right]$$

The prototype we studied does not have a device for measuring the mass of condensate, which is why we used A. Errougani's correlation for estimating the mass of adsorbed water m_{ad}. Errougani's correlation for estimating the mass of adsorbed water m_{ad} given by the relation [4]:

$$\log(m_{ad}) = 2{,}44859 \log(\frac{I_g}{T_{amb}}) - 4{,}08861$$

2. Experimental results and discussion

2.1. Solar radiation

Figure 4 shows variations in daily solar radiation over three days as a function of time. The figure shows that solar radiation starts to increase as soon as the sun rises, reaching its maximum value between 576.45 and 733.38 W/m2 in the middle of the day between 11am and 1pm; it then decreases beyond this period to reach zero around 6pm. The low level of sunshine in the middle of the day on 01/07/2017 is linked to the passage of thunderstorms.

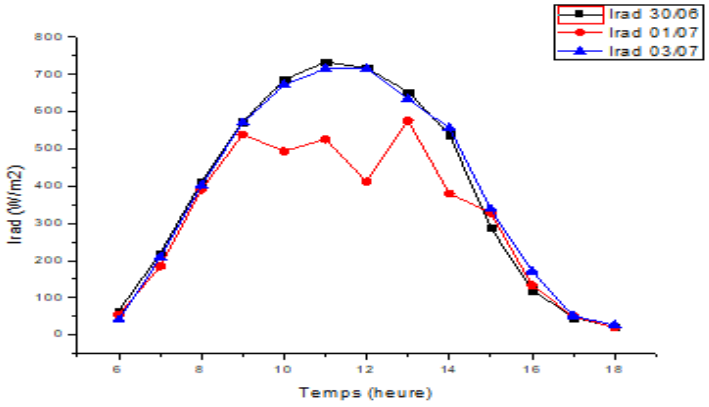

Figure 4: Sunshine

2.2. Temperature profile in the collector

Figure 5 shows the temperature profile of the solar collector as a function of time for different test days. It can be seen that the temperature profile follows the same pattern as solar radiation. The maximum collector temperature values obtained ranged from 67.13°C to 78°C on these test days. The collector temperature remained constant throughout the heating period from 11am to 1pm. After the temperature peak, there was a gradual drop in collector temperature as radiation levels fell.

A similar trend in collector temperature evolution was observed by author F. BOUZEFFOUR [3]. For this author, the maximum temperature values obtained in the adsorbent bed range from 100°C to 119°C. What's more, for this author, the maximum temperature of the adsorbent bed remained constant during the heating period from 12 h to 14 h, corresponding to the maximum intensity of solar radiation. It should be noted, however, that the maximum temperature values in the adsorbent bed of F. BOUZEFFOUR [3] are higher than those obtained in our study. This suggests that the reflective surface is conducive to increasing the temperature in the adsorbent bed in the study by F. BOUZEFFOUR [3].

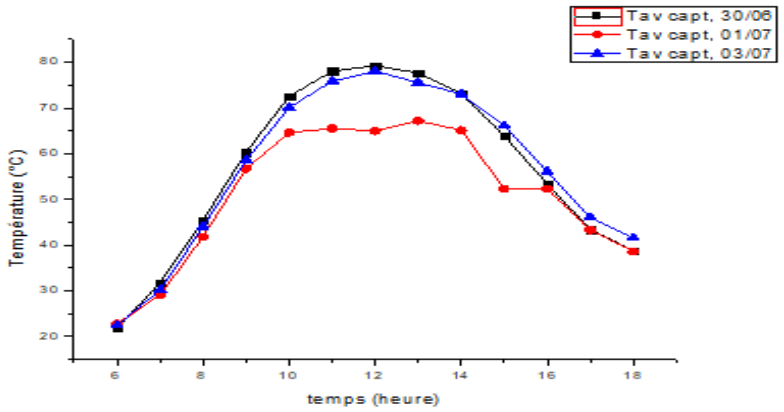

Figure 5: Temperature profile in sensor

2.3.Condenser temperature profile

Figure 6 shows the evolution of condenser temperature and ambient temperature as a function of time for the three days 30/06, 01/07 and 03/07/2017. It can be seen that the condenser temperature rises faster than the ambient temperature, reaching a maximum value of 48.4°C; 44.4°C and 47°C between 8am and 10am.

This could be explained by the desorption process. Indeed, the desorption process creates a pressure rise that drives the water vapor towards the condenser. The condensation temperature rises progressively as a result of the increase in water vapor temperature during the period from 6 a.m. to 2 p.m.

After 14 o'clock, the collector temperature falls as solar radiation decreases, leading to a drop in condenser temperature. Under these conditions, the flow of water vapor through the condenser is at its lowest, and cancels out when the condenser temperature becomes equivalent to the ambient temperature. This similar trend in condenser temperature evolution was observed experimentally by author F. BOUZEFFOUR [3]. However, for this author, the evolution of the condensation temperature was represented over the time period from 9 a.m. to 2 p.m. and the maximum temperatures obtained in the condenser ranged from 45 to 53°C.

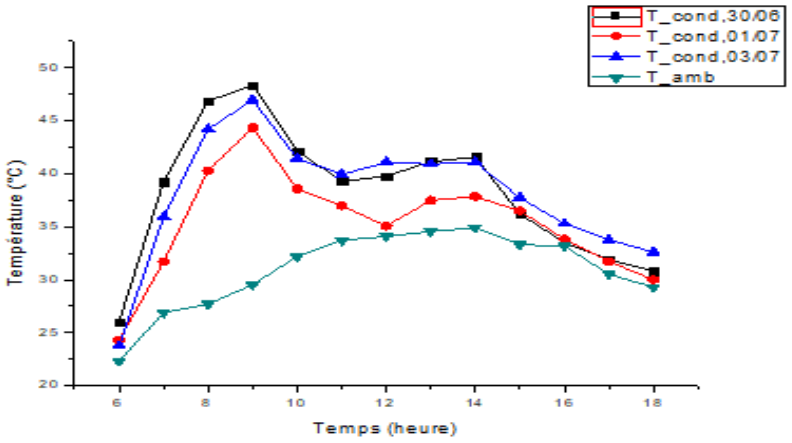

Figure 6 : Condenser temperature profile

2.4. Evaporator and storage tank temperature profile

The evaporator temperature profile curves for 06/30, 07/01 and 07/03/2017 are shown in Figure 7. This figure shows the evolution of the evaporator temperature over three days as a function of time. It can be seen that the evaporator temperature rises over the three test days, reaching a respective maximum value of 16.3 0C, 13.37 °C and 13.55 °C at 6 pm. This increase in evaporator temperature is due to the fact that the cold room in our system is not airtight.

Also, after 6 p.m., the evaporator temperature drops to a minimum value of between 9.8°C and 11.8°C on test days. During the evaporation-adsorption phase (from 6 p.m. to 4 a.m.), a certain amount of cold is produced by the evaporation of water at low pressure. It is important to note that: (i) water vapor adsorption increases with the absorbent's absorption capacity; (ii) cold production in the chamber becomes significant as water vaporization continues. A similar trend was observed by author F. BOUZEFFOUR [3]. According to this author, cold production occurs between 4.40 p.m. and 4 a.m. and the temperature obtained in the evaporator is around +6°C. This difference in evaporator temperatures is due to the fact that the cold room in our system is not very airtight, given its age (1986, when it was built).

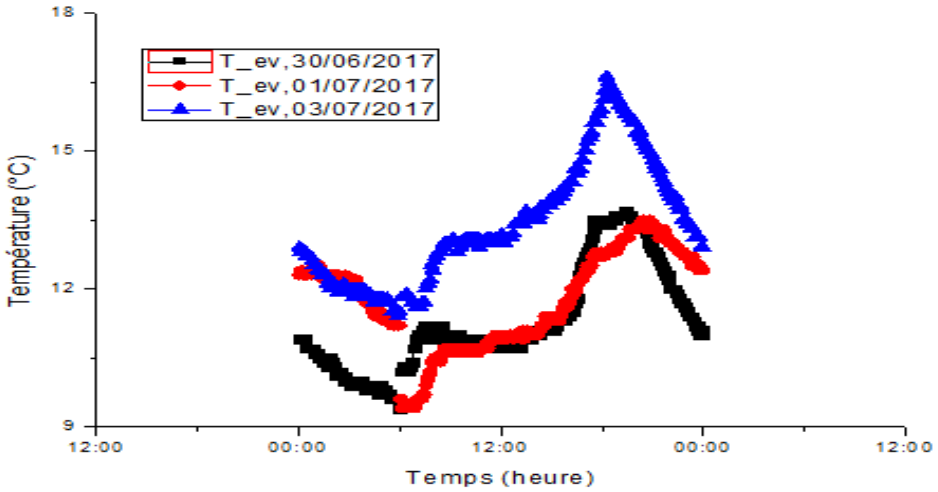

Figure 7: Temperature trends in the cold room

2.5. Prototype solar coefficient of performance

Under actual working conditions, with an average condensing temperature T_c = 51.3°C and a minimum evaporator temperature T_e = 9.4°C, the experimental COP_s of our refrigeration system ranges from 0.058 to 0.127 and the total energy received by the solar collector is between 14.56 MJ/m^2 and 18.68 MJ/m^2 as shown in Table 2.

The experimental results obtained in our study, were compared with those found in the literature as shown in Table 3. The COP_s values obtained with our device range from 0.091 to 0.138. These results are comparable to those of other adsorption refrigeration systems using the silica gel/water couple or the activated carbon/methanol couple (Table 3). These results show that our adsorption system is still working reasonably well. Indeed, we can see that the evaporation temperature increases with the COP_s . It should be noted, however, that at the evaporation temperatures obtained ($T_e \geq 9.4$°C), we can only have cool water.

Table 2: Calculation of experimental COP_s

Date	30/06/2017	01/07/2017	02/07/2017	03/07/2017
T_{amb} (°C)	28,3	29,65	31,65	31,65
T_e(°C)	10,2	9,4	14,1	11,6
T_c(°C)	51,3	46,3	44,6	46
I(W/m^2)	419	337	456	420
E (kJ)	36194,7	29118,5	39356,9	36303,6
I_g(kJ/m^2)	18097,3	14559,3	19678,5	18151,8
I_g(W/m^2)	60,03431	48,08211	64,56189	59,55307
m_{ad}(kg)	1,84485	1,07122	2,20435	1,80885
Q_f (kJ)	4570,7021	2656,0694	5440,528	4475,3683
COP_s	0,126	0,091	0,138	0,123

Table 3: Comparison of the COP_s of some adsorption solar refrigerators.

Prototype	Couple adsorbant/adsorbat	Surface (m^2)	COP_s	Energie totale reçue	Références
Présent travail	Silicagel/eau	2	0,091-0,138	14,56-18,68 MJ/m^2	-
Boubakri et al. (1992)	AC/méthanol	2	0,12	19,54 MJ/m2	[8], [9]
Hilbrand et al. (2005)	AC/méthanol	2	0,09-0,13	19-25 MJ	[8], [10]
Pons et Guilleminot (1986)	AC/méthanol	6	0,10-0,12	16-19 MJ/j	[11]
Hildbrand et al. (2004)	Silicagel/eau	2	0,12-0,23	> 20 MJ/m^2. j	[11]

Conclusion

The study shows that this prototype has a solar coefficient of performance of between 0.091 and 0.138. This result proves that these types of refrigerators stand up better to the test of time. However, the evaporator temperature has risen by around 4°C compared with the initial value, resulting in a higher solar coefficient of performance. In other words, the higher the evaporator temperature, the higher the solar coefficient of performance.

This latter result has been proven by several simulation studies, such as those by W. CHEKIROU [12] and M. A. DJEBURET [13].

Références

[1] K. Rabhi, A. Chaouki, and H. Ben Bacha, “Dynamic simulation of a solar adsorption refrigeration system,” vol. 17, p. 541–547, 2014.

[2] L. P. NOLWENN, “Solar process for the production of low temperature cold (-28C) by solid-gas sorption,” University of Perpignan, 2005.

[3] B. Fatih, “Theme Production of solar cold by adsorption and analysis of the performance by the application of the approach of artificial neural networks”, university hassiba ben-bouali de chef, 2017.

[4] F. Lemmini and A. Errougani, “Experimentation of a solar adsorption refrigerator in Morocco,” Renew. Energy, vol. 32, no. 15, p. 2629–2641, 2007.

[5] A. Boubakri et al., “experimental study of adsorption solar powered ice in agdir (Morocco)- 2. Influence of meteorological parameters,” no. 1, p. 15–21, 1992.

[6] C. Hildbrand, O. Cherbuin, and J. Mayor, “Solar adsorption refrigeration,” pp. 1–10, 2005.

[7] F. Bouzeffour, B. Khelidj, and M. Tahar abbes, “Experimental investigation of a solar adsorption refrigeration system working with silica gel/water pair: A case study for Bou-Ismail solar data,” Sol. Energy, vol. 131, p. 165–175, 2016.

[8] A. ROUAg, “Contribution to the study of heat transfer in the heat exchangers of adsorption refrigeration machines,” Mohamed Khider-Biskra University, 2017.

[9] W. CHEKIROU, “Study and analysis of a solar adsorption refrigeration machine,” Mentouri-Constantine University, 2008.

[10] F. Buchter, P. Dind, and M. Pons, “An experimental solar-powered adsorptive refrigerator tested in Burkina-Faso,” Int. J. Refrig., vol. 26, no. 1, p. 79–86, 2003.

[11] P. Goyal, P. Baredar, A. Mittal, and A. R. Siddiqui, “Adsorption refrigeration technology - An overview of theory and its solar energy applications,” Renew. sustain. Energy Rev., vol. 53, p. 1389–1410, 2016.

[12] W. Chekirou, A. Chikouche, N. Boukheit, A. Karaali, and S. Phalippou, “Dynamic modeling and simulation of the tubular adsorber of a solid adsorption machine powered by solar energy,” Int. J. Refrig., vol. 39, p. 137–151, 2014.

[13] M. A. Djebiret, M. Ouali, M. Mokrane, N. Hatraf, and N. K. Merzouk, “Parametric Study of a Single Effect Cycle of a Refrigerating Adsorption Machine,” no. June, 2016.